On–Off-Based Secure Transmission Design With Outdated Channel State Information

Jianwei Hu, *Student Member, IEEE*, Weiwei Yang, *Member, IEEE*, Nan Yang, *Member, IEEE*, Xiangyun Zhou, *Member, IEEE*, and Yueming Cai, *Senior Member, IEEE*

***Abstract*—We design new secure on–off transmission schemes in wiretap channels with outdated channel state information (CSI). In our design, we consider not only the outdated CSI from the legitimate receiver but two distinct scenarios as well, depending on whether the outdated CSI from the eavesdropper is known at the transmitter. Under this consideration, our schemes exploit useful knowledge contained in the available outdated CSI, and based on this, the transmitter decides on whether to transmit or not. We derive new closed-form expressions for the transmission probability, the connection outage probability, the secrecy outage probability, and the reliable and secure transmission probability to characterize the achievable performance. Based on these results, we present the optimal solutions that maximize the secrecy throughput under dual connection and secrecy outage constraints. Our analytical and numerical results offer detailed insights into the design of the wiretap coding parameters and the imposed outage constraints. We further show that allowing more freedom on the codeword transmission rate enables a larger feasible region of the dual outage constraints by exploiting the tradeoff between reliability and security.**

***Index Terms*—On–off scheme, outage constraints, outdated channel state information (CSI), secrecy throughput, secure transmission.**

I. Introduction

THE inherent openness of the wireless medium makes wireless data transmission difficult to shield from unintended recipients. As such, secure transmission over wireless channels becomes a critical issue in the design of wireless networks. Traditionally, security is viewed as an independent feature guaranteed through higher layer techniques, e.g., cryptographic protocols, assuming that an error-free physical-layer link has already been established [1]. In large-scale dynamic wireless networks, however, the high complexity of key distribution and management makes it difficult to achieve the required security level with cryptographic methods alone [2]. In contrast to cryptographic protocols, physical-layer security exploits the statistics of the channel at the physical layer to protect wireless transmission against eavesdropping [3], [4]. Therefore, it has been widely recognized as a complement to cryptographic protocols for security enhancement and, thus, has attracted enormous research efforts recently.

A. Background

The information-theoretic foundation of physical-layer security was laid down by Shannon's definition of perfect secrecy in [5]. Based on the work in [5], Wyner [6] introduced the wiretap channel model as a basic framework for physical-layer security. The results in [6] were subsequently generalized to the broadcast channel and the Gaussian channel in [7] and [8], respectively. These early studies revealed that if the eavesdropper's observation is a degraded version of the legitimate user's observation, it is possible to provide information-theoretically secure communication between the legitimate users while keeping the eavesdropper completely ignorant of secure messages.

A key assumption underpinning the information-theoretic contributions in [6]–[8] is that perfect channel state information (CSI) from both the legitimate receiver and the eavesdropper is available at the transmitter. However, this assumption may not be realistic since the uncertainty in CSI is a common factor that affects the performance of practical communication systems. In particular, if the eavesdropper is a passive user, knowing the CSI from the eavesdropper is almost impossible. Moreover, perfect knowledge of the legitimate user's channel may not be easy to obtain at the transmitter in practice, due to the limitations incurred by signal processing techniques, such as channel estimation errors, finite-rate feedback links, and outdated CSI (or delayed CSI).

Against this background, a growing body of research efforts has recently been devoted to examining the impact of imperfect CSI on physical-layer security. Considering the practical passive eavesdropping scenario, in [9]–[13], transmit antenna selection schemes are proposed to enhance security in wiretap channels. Considering Gaussian-distributed errors produced by imperfect channel estimation at the legitimate receiver, the authors in [14]–[19] designed secure transmission schemes and investigated the achievable performance. It is worth mentioning that He and Zhou in [19] successfully introduced on–off design to develop fixed-rate and variable-rate secure transmission schemes in the presence of channel estimation errors. Considering limited feedback constraints,

Manuscript received April 20, 2015; revised July 22, 2015; accepted September 2, 2015. Date of publication September 9, 2015; date of current version August 11, 2016. The work of J. Hu, W. Yang, and Y. Cai was supported in part by the National Natural Science Foundation of China under Grant 61371122, Grant 61471393, and Grant 61501512 and in part by the Jiangsu Provincial National Science Foundation under Grant BK20150718. The work of N. Yang and X. Zhou was supported by the Australian Research Council Discovery Project under Grant DP150103905. The review of this paper was coordinated by Dr. L. Zhao.

J. Hu, W. Yang, and Y. Cai are with the College of Communications Engineering, PLA University of Science and Technology, Nanjing 210007, China (e-mail: hujianwei1990@yeah.net; wwyang1981@163.com; caiym@vip.sina.com).

N. Yang and X. Zhou are with the Research School of Engineering, Australian National University, Canberra, ACT 0200, Australia (e-mail: nan.yang@anu.edu.au; xiangyun.zhou@anu.edu.au).

Digital Object Identifier 10.1109/TVT.2015.2477427

in [20]–[24], the secrecy performance in multiantenna systems is characterized, and the optimal power allocation applied in artificial-noise-aided beamforming is studied. Note that Zhang *et al.* in [24] also adopted an on–off design to develop the optimized artificial-noise-aided transmission scheme in limited feedback channels. In [9]–[24], although signal processing techniques with passive eavesdropping, imperfect channel estimation, and limited feedback constraints have been developed, the models and methods used in the aforementioned papers cannot be used to address another practical environment where imperfect CSI is caused by the time delay of the feedback link. This motivates us to develop new models and methods for physical-layer security with outdated CSI.

B. Motivation

Outdated CSI is a practical contributor to the uncertainty of channel knowledge at communication nodes. In a practical system with feedback delay from the receiver to the transmitter, the CSI obtained at the transmitter may be an outdated version of the actual CSI. As such, the obtained CSI cannot be directly used for secure transmission. Along this line, there are limited studies in the literature [25], [26]. Specifically, Yang *et al.* in [25] derived an upper bound on the secrecy rate loss by exploiting the Gauss–Markov fading spectrum to model the feedback delay, whereas Ferdinand *et al.* in [26] analyzed the effects of outdated CSI on the secrecy outage performance of multiple-input–single-output wiretap channels with transmit antenna selection. Notably, the studies in [25] and [26] merely concentrated on secrecy performance analysis but have not presented detailed transmission design in the presence of outdated CSI.

It is well to be reminded that although the outdated CSI is not equivalent to the actual CSI, the temporal correlation between outdated CSI and actual CSI makes it possible for the transmitter to exploit some knowledge offered by the outdated CSI to perform secure transmission. Therefore, there arises a significant problem to be addressed: *"How can we take advantage of this benefit to design secure transmission schemes?"* Recall that the on–off design, as an efficient approach that guarantees transmission quality, has been successfully used to develop transmission schemes in the presence of channel estimation errors [19] and limited feedback constraints [24], respectively. Motivated by this, in this work, we adopt the on–off design to develop secure transmission schemes in the presence of outdated CSI.

C. Contributions

We develop new secure transmission schemes in the presence of outdated CSI by using the on–off design to exploit the useful information in the outdated CSI. These schemes are designed for two distinct scenarios, depending on whether the eavesdropper is a legitimate user served by the transmitter. In *Scenario 1*, the eavesdropper is an active user (but not the intended receiver), and the outdated CSI from both the legitimate receiver and the eavesdropper is available at the transmitter. In *Scenario 2*, the eavesdropper is not a legitimate user, and only the outdated CSI from the legitimate receiver is available at the transmitter. The on–off design adopted in our developed schemes allows transmission only when the channel qualities known at the transmitter satisfy some predetermined requirements [9], [24], [27], [28]. The rationale behind the on–off design is that transmission should be avoided when the quality of the intended receiver's channel is poor or when the quality of the eavesdropper's channel is strong.

Our primary contributions are summarized as follows.

- We design new on–off transmission schemes in the presence of outdated CSI and then derive new closed-form expressions for the connection outage probability, the secrecy outage probability, and the reliable and secure transmission probability to quantify the achievable performance. Different from the studies in [19], [24], and [28], for the first time, we incorporate the reliable and secure transmission probability into the formulation of the throughput, forming the *secrecy throughput*. Notably, the secrecy throughput measures the average rate of the message that is successfully decoded at the legitimate receiver while being kept confidential to the eavesdropper.
- We determine new rate selection strategies that exploit the useful information in the outdated CSI. In these strategies, the codeword transmission rate is adaptively designed according to the feedback from the legitimate receiver. The secrecy rate is optimally selected to maximize the secrecy throughput subject to the constraints on the connection outage probability and the secrecy outage probability. We present the optimal design for both *Scenario 1* and *Scenario 2*.
- We reach an important conclusion that allowing more freedom on the codeword transmission rate enables the enhancement of the reliability level by exploiting the tradeoff between reliability and security, since the codeword transmission rate without optimization leads to poor reliability performance. We further show that this tradeoff provides us with a profound extension in the feasible region of the reliability constraint.

D. Organization

The remainder of this paper is organized as follows. Section II details the outdated CSI model, the on–off transmission schemes, and the wiretap code design in wiretap channels. In Section III, we derive the exact expressions for the performance metrics and offer numerical results to investigate the secrecy performance. In Section IV, the optimized secrecy rates for each scenario are presented, and the illustrative numerical results are provided. Some discussions and concluding remarks are provided in Sections V and VI, respectively.

II. Secure Transmission in the Presence of Outdated Channel State Information

We consider a wiretap channel where the message transmitted from a source Alice to a destination Bob is intercepted by an eavesdropper Eve. We assume that Alice, Bob, and Eve are

each equipped with a single antenna. Throughout this paper, we refer to the Alice–Bob channel as the main channel and to the Alice–Eve channel as the eavesdropper's channel. We assume that both channels are subject to Rayleigh fading. We also assume independent but nonidentical distributions between the main channel and the eavesdropper's channel such that they have different average signal-to-noise ratios (SNRs).

Prior to data transmission, Alice requests Bob to feed back his instantaneous channel quality by sending pilot signals. Aided by the pilot signals, Bob estimates the main channel coefficient, i.e., h_b, and calculates the instantaneous received SNR as $\gamma_b = P_b|h_b|^2/\sigma_b^2$, where P_b and σ_b^2 denote the average received signal power at Bob and the additive white Gaussian noise (AWGN) power at Bob, respectively, whereas Eve estimates the eavesdropper's channel coefficient, i.e., h_e, and calculates the instantaneous received SNR as $\gamma_e = P_e|h_e|^2/\sigma_e^2$, where P_e and σ_e^2 denote the average received signal power at Eve and the AWGN power at Eve, respectively. Then, Bob feeds back γ_b to Alice to facilitate wiretap code design. Whether or not Eve feeds back γ_e depends on whether Eve is an active user of the network. Specifically, we consider two scenarios based on the availability of γ_e in this work, as follows.

- *Scenario 1*: Eve is a nonpassive eavesdropper such that γ_e is fed back to Alice. This scenario represents the case where Eve is an active user of the network but is treated as a malicious eavesdropper when Alice performs secure transmission to Bob [29]–[31].
- *Scenario 2:* Eve is a passive eavesdropper such that γ_e is not fed back to Alice. This scenario represents the case where Eve is an illegitimate user of the network [9]–[13].

We clarify that in both scenarios, Eve is a regular user served by Alice, and thus, Eve's distance from Alice and the path-loss exponent are known. That is, Alice always knows the average received SNR at Eve, i.e., $\bar{\gamma}_e$. Based on the feedback information, Alice calculates the instantaneous channel capacity of the main channel during pilot transmission as $C_b = \log_2(1+\gamma_b)$. Moreover, in *Scenario 1*, Alice calculates the instantaneous channel capacity of the eavesdropper's channel capacity as $C_e = \log_2(1+\gamma_e)$, whereas in *Scenario 2*, Alice calculates the average channel capacity of the eavesdropper's channel capacity as $\bar{C}_e = \log_2(1+\bar{\gamma}_e)$. Then, Alice adaptively designs the wiretap codes based on C_b and C_e in *Scenario 1* and based on C_b and $\bar{C}_e$ in *Scenario 2*.

A. Outdated CSI

In this paper, we concentrate on the practical wiretap channel where the CSI obtained at Alice is outdated. In practice, the process of acquiring CSI at the transmitter may take a significant time duration for pilot transmission, channel estimation, and CSI feedback. This results in the fact that the channel coefficients during data transmission are not h_b and h_e. As such, the CSI obtained at Alice is an imprecise version of the actual CSI, which causes the uncertainty in channel quality.

We first describe the uncertainty in the channel knowledge obtained at Alice in the wiretap channel. We define $\tilde{h}_b$ and $\tilde{h}_e$ as the τ_d time-delayed versions of h_b and h_e, respectively. Using a Gauss–Markov process [32], we formulate $\tilde{h}_b$ and $\tilde{h}_e$ as

$$\tilde{h}_b = \rho_b h_b + \sqrt{1-\rho_b^2}w_b \tag{1}$$

$$\tilde{h}_e = \rho_e h_e + \sqrt{1-\rho_e^2}w_e \tag{2}$$

respectively, where $w_b \sim \mathcal{CN}(0,1)$ and $w_e \sim \mathcal{CN}(0,1)$ are the channel-independent errors in the main channel and the eavesdropper's channel, respectively. Here, ρ_b denotes the correlation coefficient between $\tilde{h}_b$ and h_b, whereas ρ_e denotes the correlation coefficient between $\tilde{h}_e$ and h_e. In Clark's fading model, ρ_b and ρ_e can be expressed as $\rho_b = J_0(2\pi f_b \tau_d)$ and $\rho_e = J_0(2\pi f_e \tau_d)$, where $J_0(\cdot)$ is the zeroth-order Bessel function of the first kind, and f_b and f_e are the maximum Doppler frequencies at Bob and Eve, respectively. In the Gaussian fading model, ρ_b and ρ_e can be expressed as $\rho_b = \exp(-\pi^2 f_b^2 \tau_d^2)$ and $\rho_e = \exp(-\pi^2 f_e^2 \tau_d^2)$, from which we find that ρ_b and ρ_e monotonically degrade to zero as τ_d increases. Since Jakes' model is widely adopted in the existing studies on mobile radios [32], in this work, we use this model to perform the simulations in Sections III-C, IV-C, and V. Therefore, the received signals at Bob and Eve during data transmission are given by

$$y_b = \tilde{h}_b\sqrt{P_b}x + n_b = \left(\rho_b h_b + \sqrt{1-\rho_b^2}w_b\right)\sqrt{P_b}x + n_b \tag{3}$$

$$y_e = \tilde{h}_e\sqrt{P_e}x + n_e = \left(\rho_e h_e + \sqrt{1-\rho_e^2}w_e\right)\sqrt{P_e}x + n_e \tag{4}$$

respectively, where $n_b \sim \mathcal{CN}(0,\sigma_b^2)$ and $n_e \sim \mathcal{CN}(0,\sigma_e^2)$ denote the AWGN at Bob and Eve, respectively. Based on (3) and (4), the instantaneous SNRs at Bob and Eve during data transmission are given by $\tilde{\gamma}_b = |\tilde{h}_b|^2 P_b/\sigma_b^2$ and $\tilde{\gamma}_e = |\tilde{h}_e|^2 P_e/\sigma_e^2$, respectively. Of course, $\tilde{\gamma}_b$ and $\tilde{\gamma}_e$ cannot be obtained at Alice.

B. On–Off Schemes and Performance Metrics

We adopt Wyner's encoding strategy [6] for secure transmission in the presence of outdated CSI. Before each transmission block, Alice needs to choose two rate parameters for wiretap code design, i.e., the codeword transmission rate, i.e., R_b, and the secrecy rate, i.e., R_s. The rate redundancy, i.e., $R_b - R_s$, provides secrecy against eavesdropping. We clarify that R_b and R_s hold constant over the duration of a block. In this paper, we use on–off schemes for *Scenario 1* and *Scenario 2*, as done in [19], [28], which are detailed as follows.

- On–off scheme for *Scenario 1*: Based on the feedback from Bob and Eve, Alice obtains the channel capacity of the main channel C_b and the channel capacity of the eavesdropper's channel C_e. As such, Alice uses C_b and C_e to design wiretap codes and performs data transmission only when $C_b - C_e > R_s$.
- On–off scheme for *Scenario 2*: Based on the feedback from Bob, Alice only obtains C_b. With statistic knowledge of the eavesdropper's channel, Alice uses C_b and $\bar{C}_e$ to design wiretap codes and performs data transmission only when $C_b - \bar{C}_e > R_s$.

It is worthwhile to note that perfect connection and perfect secrecy between Alice and Bob cannot be guaranteed in the presence of outdated CSI for both cases. This is due to the uncertainty in channel knowledge, i.e., Alice has no knowledge of the actual main channel capacity given by $\tilde{C}_b = \log_2(1+\tilde{\gamma}_b)$ and the actual eavesdropper's channel capacity given by $\tilde{C}_e = \log_2(1+\tilde{\gamma}_e)$. As such, the connection outage occurs when $\tilde{C}_b < R_b$, in which Bob is unable to decode the received codewords correctly. Mathematically, the connection outage probability, i.e., p_{co}, is defined as [19, eq. (16)]

$$p_{co} = \Pr\{\tilde{C}_b < R_b | \text{transmission}\}. \tag{5}$$

Moreover, the secrecy outage occurs when $R_b - R_s < \tilde{C}_e$. Mathematically, the secrecy outage probability, i.e., p_{so}, is defined as [19, eq. (15)]

$$p_{so} = \Pr\{R_b - R_s < \tilde{C}_e | \text{transmission}\}. \tag{6}$$

Note that both outage probabilities are conditioned upon a message being transmitted. These outage probabilities are of practical importance since the reliability level and the security level can be measured using these probabilities when the outdated CSI is present. However, from (5) and (6), we find that the connection outage event and the secrecy outage event are definitely not independent from each other but related with R_b. To evaluate the combination of reliability and security, we resort to the successful (reliable and secure) transmission probability, i.e., $p_{\rm rst}$, which is defined as

$$p_{\rm rst} = \Pr\{\tilde{C}_b \geq R_b, R_b - R_s \geq \tilde{C}_e | \text{transmission}\}. \tag{7}$$

Notably, (7) is a novel formulation to characterize the reliability and security levels of transmission.

C. Rate Selection Strategy

To exploit the useful knowledge in the outdated CSI, the strategy for the choice of R_b and R_s is explained as follows: R_b is adaptively designed according to the feedback from the legitimate receiver, whereas R_s is optimally chosen and keeps constant over the transmission block. In other words, this is an adaptive-codeword-transmission-rate but fixed-secrecy-rate strategy. Since C_b is the only knowledge obtained from Bob, it is convenient and natural for Alice to set $R_b = C_b$ to guarantee maximum rate redundancy against eavesdropping. This leads to the fact that R_s is the only controllable parameter in the wiretap code design. As such, R_s is optimally chosen before data transmission and then kept constant during data transmission.

The aim of our design is to achieve the optimal secrecy throughput under the constraints of two outage probabilities. Here, the secrecy throughput, i.e., η, is defined as

$$\eta = p_{tx} p_{\rm rst} R_s \tag{8}$$

where p_{tx} denotes the transmission probability, and $p_{\rm rst}$ is given by (7). *We highlight that the secrecy throughput in* (8) *is different from the throughput in* [19], *which is defined as* $p_{tx}(1-p_{co})R_s$. In (8), we introduce $p_{\rm rst}$ into the formulation of the secrecy throughput. We clarify that the incorporation of $p_{\rm rst}$ is reasonable and necessary for the assessment and improvement of reliability and security. Specifically, $p_{\rm rst}$ jointly quantizes the reliability level and the security level of the secrecy throughput.

Using (8), our design aim is formulated as

$$\begin{aligned} \max_{R_s} \quad & \eta \\ \text{subject to} \quad & p_{co} \leq \epsilon, p_{so} \leq \delta \end{aligned} \tag{9}$$

where ϵ denotes the reliability constraint, and δ denotes the security constraint. Note that solving the optimized R_s in (9) can help us not only obtain good secrecy throughput performance but keep the reliability and security levels under control as well.

III. Secrecy Performance With On–Off Transmission Schemes

Here, we analyze the secrecy performance for the two scenarios presented in Section II-B by exploiting the on–off transmission schemes. Specifically, we derive the closed-form expressions for the connection outage probability, the secrecy outage probability, and the reliable and secure transmission probability defined in Section II-B. We then present the numerical results to examine the performance of the on–off transmission schemes with outdated CSI.

A. Performance Analysis for Scenario 1

Here, we consider *Scenario 1* and derive new expressions for the connection outage probability, the secrecy outage probability, and the reliable and secure transmission probability. We then present the feasibility of the reliability constraint and the security constraint.

1) $p_{tx_1}(R_s)$, $p_{co_1}(R_s)$, $p_{so_1}(R_s)$, and $p_{\rm rst_1}(R_s)$: In *Scenario 1*, Alice sets $R_b = C_b$ and performs data transmission only when $C_b - C_e \geq R_s$. The transmission probability in *Scenario 1* is derived as

$$\begin{aligned} p_{tx_1}(R_s) &= \Pr\{C_b - C_e \geq R_s\} \\ &= \Pr\{\gamma_b \geq 2^{R_s}(1+\gamma_e) - 1\} \\ &= \int_0^\infty f_{\gamma_e}(\gamma_e) \left(\int_{2^{R_s}(1+\gamma_e)-1}^\infty f_{\gamma_b}(\gamma_b) d\gamma_b \right) d\gamma_e \\ &= \frac{\bar{\gamma}_b}{\bar{\gamma}_b + 2^{R_s}\bar{\gamma}_e} \exp\left(-\frac{2^{R_s}-1}{\bar{\gamma}_b} \right). \end{aligned} \tag{10}$$

We note that (10) can be obtained by using the probability density functions (pdfs) of γ_b and γ_e. In this paper, we assume that both the main channel and the eavesdropper's channel are subject to Rayleigh fading, such that the pdf of γ_b is $f_{\gamma_b}(\gamma_b) = \exp(-\gamma_b/\bar{\gamma}_b)/\bar{\gamma}_b$ and the pdf of γ_e is $f_{\gamma_e}(\gamma_e) = \exp(-\gamma_e/\bar{\gamma}_e)/\bar{\gamma}_e$ [19], where $\bar{\gamma}_b = \mathbb{E}[h_b^2]P_b/\sigma_b^2$ denotes the average SNR at Bob, and $\bar{\gamma}_e = \mathbb{E}[h_e^2]P_e/\sigma_e^2$ denotes the average SNR at Eve.

The connection outage occurs when $\tilde{C}_b < C_b$. As such, the connection outage probability in *Scenario 1* is given by

$$p_{co_1}(R_s) = \Pr\{\tilde{C}_b < C_b | C_b - C_e \geq R_s\}. \quad (11)$$

Based on the cumulative distribution function (cdf) of a non-central chi-square-distributed variable, we derive $p_{co_1}(R_s)$ as

$$\begin{aligned} p_{co_1}(R_s) = 1 &- \frac{\bar{\gamma}_b + 2^{R_s}\bar{\gamma}_e}{\bar{\gamma}_b} \exp\left(-\frac{\left(1+\rho_b^2\right)\left(2^{R_s}-1\right)}{\left(1-\rho_b^2\right)\bar{\gamma}_b}\right) \\ &\times \sum_{n=0}^{\infty}\sum_{k=0}^{\infty} \frac{\rho_b^{2(n+k)}\left(1-\rho_b^2\right)\Gamma(n+2k+1)}{k!2^{n+2k+1}\Gamma(n+k+1)} \\ &\times \sum_{m=0}^{n+2k}\sum_{q=0}^{m} \frac{\left(2^{R_s}-1\right)^{m-q}2^{m+qR_s}}{(m-q)!\left(\left(1-\rho_b^2\right)\bar{\gamma}_b\right)^m\bar{\gamma}_e} \\ &\times \left(\frac{\left(1-\rho_b^2\right)\bar{\gamma}_b\bar{\gamma}_e}{\left(1-\rho_b^2\right)\bar{\gamma}_b + 2^{R_s+1}\bar{\gamma}_e}\right)^{q+1} \end{aligned} \quad (12)$$

where $\Gamma(\cdot)$ is the Gamma function defined in [33, eq. (8.310.1)]. The proof is given in Appendix A.

The secrecy outage occurs when $C_b - R_s < \tilde{C}_e$. As such, the secrecy outage probability in *Scenario 1* is given by

$$p_{so_1}(R_s) = \Pr\{C_b - R_s < \tilde{C}_e | C_b - C_e \geq R_s\}. \quad (13)$$

We derive $p_{so_1}(R_s)$ as

$$p_{so_1}(R_s) = \frac{\bar{\gamma}_b + 2^{R_s}\bar{\gamma}_e}{\bar{\gamma}_b} \exp\left(\frac{2^{R_s}-1}{\bar{\gamma}_b}\right)(\ell_1 - \ell_2) \quad (14)$$

where ℓ_1 is

$$\begin{aligned} \ell_1 = \exp&\left(-\frac{2^{-R_s}-1}{\left(1-\rho_e^2\right)\bar{\gamma}_e}\right)\sum_{n=0}^{\infty}\sum_{k=0}^{\infty}\frac{\rho_e^{2(n+k)}\left(1-\rho_e^2\right)}{\Gamma(k+1)\left(\left(1-\rho_e^2\right)\bar{\gamma}_e\right)^k} \\ &\times \sum_{q=0}^{k}\binom{k}{q}\frac{\left(1-2^{R_s}\right)^{k-q}}{2^{kR_s}\bar{\gamma}_b}\left(\frac{\left(1-\rho_e^2\right)2^{R_s}\bar{\gamma}_b\bar{\gamma}_e}{\bar{\gamma}_b + \left(1-\rho_e^2\right)2^{R_s}\bar{\gamma}_e}\right)^{q+1} \\ &\times \Gamma\left(q+1, \frac{\bar{\gamma}_b + \left(1-\rho_e^2\right)2^{R_s}\bar{\gamma}_e}{\left(1-\rho_e^2\right)2^{R_s}\bar{\gamma}_b\bar{\gamma}_e}(2^{R_s}-1)\right) \end{aligned} \quad (15)$$

ℓ_2 is

$$\begin{aligned} \ell_2 = \exp&\left(-\frac{2^{1-R_s}-2}{\left(1-\rho_e^2\right)\bar{\gamma}_e}\right)\sum_{n=0}^{\infty}\sum_{k=0}^{\infty}\frac{\rho_e^{2(n+k)}\left(1-\rho_e^2\right)}{k!\left(\left(1-\rho_e^2\right)\bar{\gamma}_e\right)^k} \\ &\times \sum_{m=0}^{n+k}\sum_{q=0}^{k+m}\binom{k+m}{q}\frac{\left(2^{-R_s}-1\right)^{k+m-q}2^{-qR_s}}{m!\left(\left(1-\rho_e^2\right)\bar{\gamma}_e\right)^m\bar{\gamma}_b} \\ &\times \Gamma\left(q+1, \frac{2^{1-R_s}\bar{\gamma}_b + \left(1-\rho_e^2\right)\bar{\gamma}_e}{\left(1-\rho_e^2\right)\bar{\gamma}_b\bar{\gamma}_e}(2^{R_s}-1)\right) \\ &\times \left(\frac{\left(1-\rho_e^2\right)\bar{\gamma}_b\bar{\gamma}_e}{2^{1-R_s}\bar{\gamma}_b + \left(1-\rho_e^2\right)\bar{\gamma}_e}\right)^{q+1} \end{aligned} \quad (16)$$

and $\Gamma(\cdot,\cdot)$ is the incomplete Gamma function defined in [33, eq. (8.352.2)]. The proof is given in Appendix B.

The successful transmission occurs when both $\tilde{C}_b \geq C_b$ and $C_b - R_s \geq \tilde{C}_e$ are simultaneously satisfied. As such, the reliable and secure transmission probability in *Scenario 1* is given by

$$p_{\mathrm{rst}_1}(R_s) = \Pr\{\tilde{C}_b \geq C_b, C_b - R_s \geq \tilde{C}_e | C_b - C_e \geq R_s\}. \quad (17)$$

We derive $p_{\mathrm{rst}_1}(R_s)$ as

$$p_{\mathrm{rst}_1}(R_s) = \frac{\bar{\gamma}_b + 2^{R_s}\bar{\gamma}_e}{\bar{\gamma}_b}\exp\left(\frac{2^{R_s}-1}{\bar{\gamma}_b}\right)(\ell_3 - \ell_4 - \ell_5) \quad (18)$$

where ℓ_3 is

$$\begin{aligned} \ell_3 = &\sum_{n=0}^{\infty}\sum_{k=0}^{\infty}\frac{\rho_b^{2(n+k)}\left(1-\rho_b^2\right)}{\Gamma(k+1)\Gamma(n+k+1)2^{n+2k+1}} \\ &\times \Gamma\left(n+2k+1, \frac{2(2^{R_s}-1)}{\left(1-\rho_b^2\right)\bar{\gamma}_b}\right) \end{aligned} \quad (19)$$

ℓ_4 is

$$\begin{aligned} \ell_4 = &\exp\left(-\frac{2^{-R_s}-1}{\bar{\gamma}_e}\right)\sum_{n=0}^{\infty}\sum_{k=0}^{\infty}\frac{\rho_b^{2(n+k)}\left(1-\rho_b^2\right)}{\Gamma(k+1)\Gamma(n+k+1)} \\ &\times \Gamma\left(n+2k+1, \frac{\left(2^{R_s+1}\bar{\gamma}_e + \left(1-\rho_b^2\right)\bar{\gamma}_b\right)}{\left(2^{R_s}-1\right)^{-1}\left(1-\rho_b^2\right)2^{R_s}\bar{\gamma}_b\bar{\gamma}_e}\right) \\ &\times \left(\frac{2^{R_s}\bar{\gamma}_e}{2^{R_s+1}\bar{\gamma}_e + \left(1-\rho_b^2\right)\bar{\gamma}_b}\right)^{n+2k+1} \end{aligned} \quad (20)$$

and $\ell_5 = \ell_6 - \ell_7$, where ℓ_6 and ℓ_7 are given, respectively, in (21) and (22), shown at the bottom of the next page. The proof is given in Appendix C.

Remark 1: We clarify that the connection outage probability is merely affected by ρ_b, as indicated by (12), and the secrecy outage probability is merely affected by ρ_e, as indicated by (14). This reveals that in *Scenario 1*, the reliability level depends on the outdated CSI of the main channel, whereas the security level depends on the outdated CSI of the eavesdropper's channel.

2) Feasibility of Constraints: We now investigate the feasibility of the reliability constraint and the security constraint. Using the mathematical software package to take the first derivative of $p_{co_1}(R_s)$ in (12), we find that $p_{co_1}(R_s)$ is an increasing function of R_s. When $R_s \to 0$, $p_{co_1}(R_s)$ achieves its lower bound, i.e., $p_{co_1,LB}$. We obtain $p_{co_1,LB}$ as

$$\begin{aligned} p_{co_1,LB} = 1 &- \sum_{n=0}^{\infty}\sum_{k=0}^{\infty}\frac{\rho_b^{2(n+k)}\Gamma(n+2k+1)}{\Gamma(k+1)\Gamma(n+k+1)2^{n+2k+1}} \\ &\times \sum_{n=0}^{n+2k}\frac{\left(1-\rho_b^2\right)^2(\bar{\gamma}_b + \bar{\gamma}_e)2^m\bar{\gamma}_e^m}{\left(2\bar{\gamma}_e + \left(1-\rho_b^2\right)\bar{\gamma}_b\right)^{m+1}}. \end{aligned} \quad (23)$$

As such, the feasible range of the reliability constraint in *Scenario 1* is given by

$$p_{co_1,LB} < \epsilon \leq 1. \quad (24)$$

We then take the first derivative of $p_{so_1}(R_s)$ in (14) and find that $p_{so_1}(R_s)$ is also an increasing function of R_s. When

$R_s \to 0$, $p_{so_1}(R_s)$ achieves its lower bound, i.e., $p_{so_1,LB}$. We obtain $p_{so_1,LB}$ as

$$p_{so_1,LB} = \frac{\bar{\gamma}_b + \bar{\gamma}_e}{\bar{\gamma}_b} \sum_{n=0}^{\infty}\sum_{k=0}^{\infty} \left(\frac{\rho_e^{2(n+k)} \left(1-\rho_e^2\right)^2 \bar{\gamma}_e \bar{\gamma}_b^k}{\left(\bar{\gamma}_b + \left(1-\rho_e^2\right)\bar{\gamma}_e\right)^{k+1}} - \sum_{m=0}^{n+k} \binom{m+k}{m} \frac{\rho_e^{2(n+k)} \left(1-\rho_e^2\right)^2 \bar{\gamma}_e \bar{\gamma}_b^{m+k}}{\left(2\bar{\gamma}_b + \left(1-\rho_e^2\right)\bar{\gamma}_e\right)^{m+k+1}} \right). \quad (25)$$

Accordingly, we obtain the feasible range of the security constraint in *Scenario 1* as

$$p_{so_1,LB} < \delta \leq 1. \quad (26)$$

We highlight that in *Scenario 1*, the reliability constraint and the security constraint are feasible only when (24) and (26) are satisfied.

B. Performance Analysis for Scenario 2

Here, we concentrate on *Scenario 2*. New closed-form expressions are derived for the transmission probability, the connection outage probability, the secrecy outage probability, and the reliable and secure transmission probability; based on this, we evaluate the feasibility of the reliability and security constraints.

1) $p_{tx_2}(R_s)$, $p_{co_2}(R_s)$, $p_{so_2}(R_s)$, and $p_{\mathrm{rst}_2}(R_s)$: In *Scenario 2*, Alice has no knowledge of C_e. As such, Alice sets $R_b = C_b$ and performs secure transmission only when $C_b - \bar{C}_e \geq R_s$. The transmission probability in *Scenario 2* is derived as

$$\begin{aligned} p_{tx_2}(R_s) &= \Pr\{C_b - \bar{C}_e \geq R_s\} \\ &= \Pr\left\{\gamma_b \geq 2^{R_s}(1+\bar{\gamma}_e) - 1\right\} \\ &= \int_{2^{R_s}(1+\bar{\gamma}_e)-1}^{\infty} f_{\gamma_b}(\gamma_b) d\gamma_b \\ &= \exp\left(-\frac{2^{R_s}(1+\bar{\gamma}_e)-1}{\bar{\gamma}_b}\right). \end{aligned} \quad (27)$$

The connection outage probability in *Scenario 2* is given by

$$p_{co_2}(R_s) = \Pr\{\tilde{C}_b < C_b | C_b - \bar{C}_e \geq R_s\}. \quad (28)$$

Applying the cdf of a noncentral chi-square-distributed variable, $p_{co_2}(R_s)$ is derived as

$$\begin{aligned} p_{co_2}(R_s) = 1 - \exp\left(\frac{2^{R_s}(1+\bar{\gamma}_e)-1}{\bar{\gamma}_b}\right) \sum_{n=0}^{\infty}\sum_{k=0}^{\infty} \frac{1}{\Gamma(k+1)} \\ \times \Gamma\left(n+2k+1, \frac{2^{R_s+1}(1+\bar{\gamma}_e)-2}{\left(1-\rho_b^2\right)\bar{\gamma}_b}\right) \\ \times \left(\frac{1}{2}\right)^{n+2k+1} \frac{\rho_b^{2(n+k)}\left(1-\rho_b^2\right)}{\Gamma(n+k+1)}. \end{aligned} \quad (29)$$

The secrecy outage probability in *Scenario 2* is given by

$$p_{so_2}(R_s) = \Pr\{C_b - R_s < \tilde{C}_e | C_b - \bar{C}_e \geq R_s\}. \quad (30)$$

Using the statistics of γ_b and $\tilde{\gamma}_e$, we derive $p_{so_2}(R_s)$ as

$$p_{so_2}(R_s) = \frac{2^{R_s}\bar{\gamma}_e \exp -1}{2^{R_s}\bar{\gamma}_e + \bar{\gamma}_b}. \quad (31)$$

The reliable and secure transmission probability in *Scenario 2* is given by

$$p_{\mathrm{rst}_2}(R_s) = \Pr\{\tilde{C}_b \geq C_b, C_b - R_s \geq \tilde{C}_e | C_b - \tilde{C}_e \geq R_s\}. \quad (32)$$

We derive $p_{\mathrm{rst}_2}(R_s)$ as

$$p_{\mathrm{rst}_2}(R_s) = \exp\left(\frac{2^{R_s}(1+\bar{\gamma}_e)-1}{\bar{\gamma}_b}\right)(\ell_8 - \ell_9) \quad (33)$$

where ℓ_8 is

$$\begin{aligned} \ell_8 = \sum_{n=0}^{\infty}\sum_{k=0}^{\infty} \frac{\rho_b^{2(n+k)}\left(1-\rho_b^2\right)}{\Gamma(k+1)\Gamma(n+k+1)} \left(\frac{1}{2}\right)^{n+2k+1} \\ \times \Gamma\left(n+2k+1, \frac{2\left(2^{R_s}+1(1+\bar{\gamma}_e)-2\right)}{\left(1-\rho_b^2\right)\bar{\gamma}_b}\right) \end{aligned} \quad (34)$$

$$\ell_6 = \exp\left(-\frac{2^{-R_s}-1}{\left(1-\rho_e^2\right)\bar{\gamma}_e}\right) \sum_{n=0}^{\infty}\sum_{k=0}^{\infty}\sum_{s=0}^{\infty}\sum_{t=0}^{\infty} \frac{\rho_b^{2(n+k)}\rho_e^{2(s+t)}\left(1-\rho_b^2\right)\left(1-\rho_e^2\right)\left(\left(1-\rho_e^2\right)\bar{\gamma}_e\right)^{n+2k-t+1}}{k!\Gamma(n+k+1)t!\left(2\left(1-\rho_e^2\right)\bar{\gamma}_e + 2^{-R_s}\left(1-\rho_b^2\right)\bar{\gamma}_b\right)^{n+2k+1}} \sum_{q=0}^{t} \frac{t!\left(2^{-R_s}-1\right)^{t-q}}{q!(t-q)!}$$
$$\times \left(\frac{2^{-R_s}\left(1-\rho_b^2\right)\left(1-\rho_e^2\right)\bar{\gamma}_b\bar{\gamma}_e}{2\left(1-\rho_e^2\right)\bar{\gamma}_e + 2^{-R_s}\left(1-\rho_b^2\right)\bar{\gamma}_b}\right)^q \Gamma\left(n+2k+q+1, \frac{2\left(1-\rho_e^2\right)\bar{\gamma}_e + 2^{-R_s}\left(1-\rho_b^2\right)\bar{\gamma}_b}{\left(2^{R_s}-1\right)^{-1}\left(1-\rho_b^2\right)\left(1-\rho_e^2\right)\bar{\gamma}_b\bar{\gamma}_e}\right) \quad (21)$$

$$\ell_7 = \exp\left(-\frac{2^{1-R_s}-2}{\left(1-\rho_e^2\right)\bar{\gamma}_e}\right) \sum_{n=0}^{\infty}\sum_{k=0}^{\infty}\sum_{s=0}^{\infty}\sum_{t=0}^{\infty} \frac{\rho_b^{2(n+k)}\rho_e^{2(s+t)}\left(1-\rho_b^2\right)\left(1-\rho_e^2\right)}{\left(2\left(1-\rho_e^2\right)\bar{\gamma}_e + 2^{1-R_s}\left(1-\rho_b^2\right)\bar{\gamma}_b\right)^{n+2k+1}} \sum_{m=0}^{s+t}\sum_{q=0}^{t+m} \frac{\left(\left(1-\rho_e^2\right)\bar{\gamma}_e\right)^{n+2k-t-m+1}}{\Gamma(n+k+1)(t+m-q)!}$$
$$\times \frac{\left(2^{-R_s}-1\right)^{t+m-q}}{\left((t+m)!\right)^{-1}k!t!m!q!} \left(\frac{2^{-R_s}\left(1-\rho_b^2\right)\left(1-\rho_e^2\right)\bar{\gamma}_b\bar{\gamma}_e}{2\left(1-\rho_e^2\right)\bar{\gamma}_e + 2^{1-R_s}\left(1-\rho_b^2\right)\bar{\gamma}_b}\right)^q \Gamma\left(n+2k+q+1, \frac{2\left(1-\rho_e^2\right)\bar{\gamma}_e + 2^{1-R_s}\left(1-\rho_b^2\right)\bar{\gamma}_b}{\left(2^{R_s}-1\right)^{-1}\left(1-\rho_b^2\right)\left(1-\rho_e^2\right)\bar{\gamma}_b\bar{\gamma}_e}\right) \quad (22)$$

and ℓ_9 is

$$\ell_9 = \exp\left(-\frac{2^{-R_s}-1}{\bar{\gamma}_e}\right)\sum_{n=0}^{\infty}\sum_{k=0}^{\infty}\frac{\rho_b^{2(n+k)}\left(1-\rho_b^2\right)}{\Gamma(k+1)\Gamma(n+k+1)} \times \Gamma\left(n+2k+1\frac{\left(2^{R_s}+1\bar{\gamma}_e=(1-\rho_b^2)\bar{\gamma}_b\right)(\bar{\gamma}_b\bar{\gamma}_e)^{-1}}{\left(2^{R_s}(1+\bar{\gamma}_e)-1\right)^{-1}2^{R_s}(1-\rho_b^2)}\right) \times \left(\frac{2^{R_s}\bar{\gamma}_e}{2^{R_s}+1\bar{\gamma}_e+(1-\rho_b^2)\,\bar{\gamma}_b}\right)^{n+2k+1}. \quad (35)$$

Remark 2: Based on (29) and (31), we find that the connection outage probability is only affected by ρ_b but the secrecy outage probability is influenced by neither ρ_b nor ρ_e. This reveals that in *Scenario 2*, the outdated CSI only influences the reliability level.

2) Feasibility of Constraints: We then examine the feasibility of the reliability constraint and the security constraint. Using the mathematical software package to take the first-order derivative of $p_{co_2}(R_s)$ in (29), we find that $p_{co_2}(R_s)$ is an increasing function of R_s. When $R_s \to 0$, $p_{co_2}(R_s)$ achieves its lower bound, i.e., $p_{co_2,LB}$, which is derived as

$$p_{co_2,LB} = 1-\exp\left(\frac{\bar{\gamma}_e}{\bar{\gamma}_b}\right)\sum_{n=0}^{\infty}\sum_{k=0}^{\infty}\frac{\rho^{2(n+k)}(1-\rho^2)}{\Gamma(k+1)\Gamma(n+k+1)} \times\left(\frac{1}{2}\right)^{n+2k+1}\Gamma\left(n+2k+1,\frac{2\bar{\gamma}_e}{(1-\rho^2)\bar{\gamma}_b}\right). \quad (36)$$

Therefore, the feasible range of the reliability constraint in *Scenario 2* is given by

$$p_{co_2,LB} < \epsilon \leq 1. \quad (37)$$

Next, by observing (31), we see that $p_{so_2}(R_s)$ is also an increasing function of R_s. When $R_s \to 0$, $p_{so_2}(R_s)$ achieves its lower bound, i.e., $p_{so_2,LB}$, which is given by

$$p_{so_2,LB} = \frac{\bar{\gamma}_e \exp(-1)}{\bar{\gamma}_e+\bar{\gamma}_b}. \quad (38)$$

Thus, the feasible range of the security constraint in *Scenario 2* is obtained as

$$p_{so_2,LB} < \delta \leq 1. \quad (39)$$

It is worthwhile to note that in *Scenario 2*, the reliability constraint and the security constraint are feasible only when (37) and (39) are satisfied.

C. Numerical Results

We present numerical results in this section to examine the performance of the on–off transmission schemes. We clarify that the infinitive summations in our derived closed-form expressions can be perfectly approximated with finite summations (usually, the first ten terms in the summations give an accurate approximation). Unless specified otherwise, the simulation settings are as follows: The average received SNR at Bob is assumed to be $P_b/\sigma_b^2 = 10$ dB, whereas the average received SNR at Eve is assumed to be $P_e/\sigma_e^2 = 0$ dB. In each simulation trial, the main channel coefficient and the eavesdropper's channel coefficient are randomly generated using an independent and identically distributed complex Gaussian distribution with zero mean and unit variance. The temporal correlation parameters of the two channel coefficients are assumed to follow Clarke's model and are characterized by $\rho_b = J_0(2\pi f_b \tau_d)$ and $\rho_e = J_0(2\pi f_e \tau_d)$, respectively. All the results to be shown are averaged over 10 000 channel trials. It is evident in Figs. 1–3 that the Monte Carlo simulation points, marked by "*," precisely match the analytical curves, which demonstrates the accuracy of our analysis.

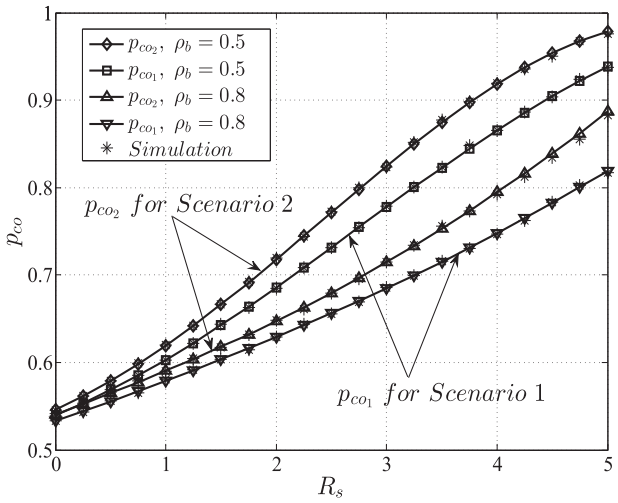

Fig. 1. Connection outage probability versus R_s with outdated CSI for $\overline{\gamma}_b = 10$ dB and $\overline{\gamma}_e = 0$ dB.

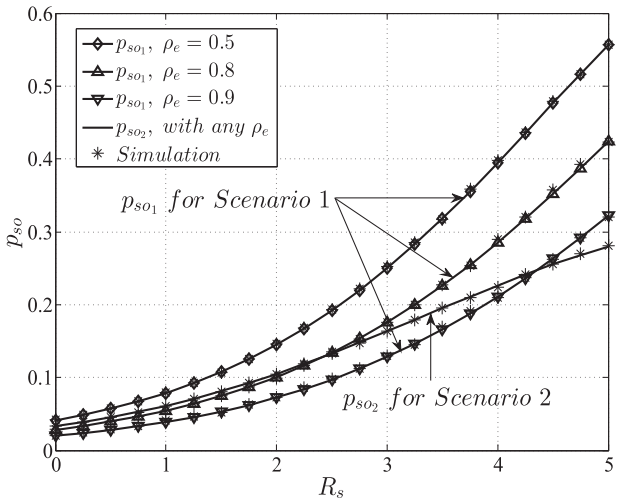

Fig. 2. Secrecy outage probability versus R_s with outdated CSI for $\overline{\gamma}_b = 10$ dB and $\overline{\gamma}_e = 0$ dB.

Fig. 1 plots the connection outage probability versus R_s for two scenarios with different values of ρ_b. In this figure, $p_{co_1}(R_s)$ and $p_{co_2}(R_s)$ are generated from (12) and (29), respectively. We first observe that $p_{co_1}(R_s)$ and $p_{co_2}(R_s)$ increase with R_s. This is due to the fact that an increasing R_s requires a higher C_b to satisfy the transmission condition. Notably, a higher C_b leads to a higher probability that $\tilde{C}_b$ is lower than C_b, due to the characteristics of the Gauss–Markov process. Second, we observe that $p_{co_1}(R_s)$ and $p_{co_2}(R_s)$

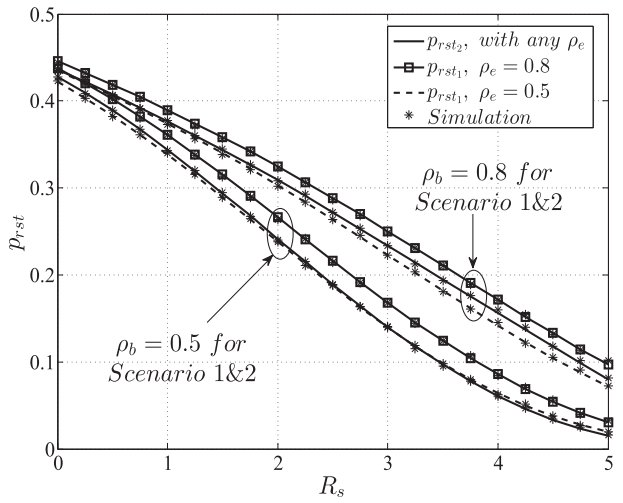

Fig. 3. Reliable and secure transmission probability versus R_s with outdated CSI for $\overline{\gamma}_b = 10$ dB and $\overline{\gamma}_e = 0$ dB.

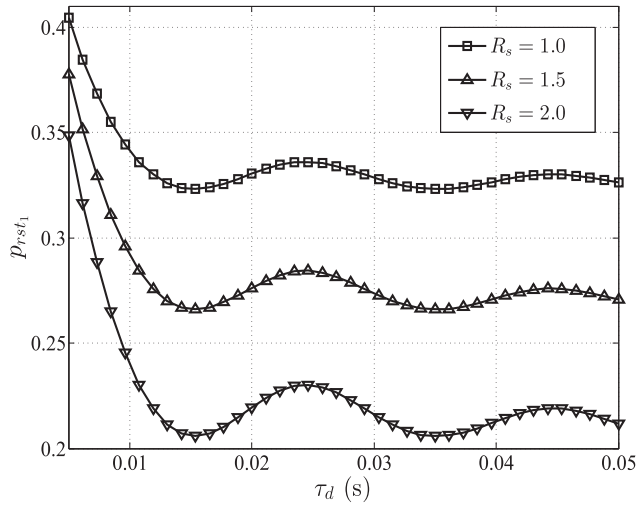

Fig. 4. Reliable and secure transmission probability versus τ_d for $\overline{\gamma}_b = 10$ dB, $\overline{\gamma}_e = 0$ dB, $v_b = v_e = 30$ km/h, and $f_c = 900$ MHz in *Scenario 1*.

increase when ρ_b decreases. This observation is not surprising since the uncertainty in the main channel quality increases as ρ_b decreases, which results in poorer reliability. Third, we observe that $p_{co_2}(R_s)$ is higher than $p_{co_1}(R_s)$ for the same ρ_b. This is due to the fact that the transmission condition in *Scenario 2*, i.e., $C_b \geq \bar{C}_e + R_s$, is stricter than that in *Scenario 1*, i.e., $C_b \geq C_e + R_s$. Thus, a higher C_b is required in *Scenario 2*, which results in worse reliability. Fourth, we observe that both $p_{co_1}(R_s)$ and $p_{co_2}(R_s)$ are always greater than 0.5, which implies that the reliability constraint should be loose in the on–off transmission schemes.

Fig. 2 plots the secrecy outage probability versus R_s for two scenarios with different values of ρ_e. In this figure, $p_{so_1}(R_s)$ and $p_{so_2}(R_s)$ are generated from (14) and (31), respectively. First, we observe that $p_{so_1}(R_s)$ and $p_{so_2}(R_s)$ increase as R_s increases. This is due to the fact that the rate redundancy, i.e., $C_b - R_s$, decreases with R_s and a lower rate redundancy leads to a higher probability that $\tilde{C}_e$ is higher than the rate redundancy. We then find that $p_{so_2}(R_s)$ is not influenced by the value of ρ_e and that different behaviors of $p_{so_1}(R_s)$ are observed, depending on the value of ρ_e, as indicated by (31). When ρ_e is not sufficiently high (e.g., $\rho_e \leq 0.5$), $p_{so_1}(R_s)$ is always higher than $p_{so_2}(R_s)$; however, when ρ_e is sufficiently high (e.g., $\rho_e > 0.9$), the opposite happens. From a design perspective, this observation implies that C_e should be used for transmission design only when ρ_e is high; otherwise, directly using $\bar{C}_e$ is a better choice for security enhancement. Moreover, we find that $p_{so_1}(R_s)$ and $p_{so_2}(R_s)$ are smaller than 0.1 for low R_s, which implies that the security constraint can be sufficiently strict in the on–off transmission schemes.

Fig. 3 plots the reliable and secrecy transmission probability versus R_s for two scenarios with different values of ρ_b and ρ_e. In this figure, $p_{\mathrm{rst}_1}(R_s)$ and $p_{\mathrm{rst}_2}(R_s)$ are generated from (18) and (33), respectively. We first observe that $p_{\mathrm{rst}_1}(R_s)$ and $p_{\mathrm{rst}_2}(R_s)$ decrease as R_s increases. This is due to the fact that increasing R_s strengthens the transmission condition (requiring higher C_b), which leads to a lower probability that $\tilde{C}_b$ is higher than C_b while the rate redundancy is higher than $\tilde{C}_e$. We also observe that $p_{\mathrm{rst}_1}(R_s)$ and $p_{\mathrm{rst}_2}(R_s)$ decrease when ρ_b decreases. Moreover, for a fixed ρ_b in *Scenario 1*, $p_{\mathrm{rst}_1}(R_s)$ also decreases when ρ_e decreases. This is because the uncertainty in the main and eavesdropper's channel quality increases as ρ_b and ρ_e decrease, which results in poorer reliability and security levels. Furthermore, we observe that for a fixed ρ_b, when ρ_e is high (e.g., $\rho_e = 0.8$), $p_{\mathrm{rst}_1}(R_s)$ is higher than $p_{\mathrm{rst}_2}(R_s)$; however, when ρ_e is low (e.g., $\rho_e = 0.5$), $p_{\mathrm{rst}_1}(R_s)$ is lower than $p_{\mathrm{rst}_2}(R_s)$. This observation demonstrates that in terms of the reliable and secrecy transmission probability, a sufficiently high ρ_e is required to guarantee that *Scenario 1* performs better than *Scenario 2*.

Fig. 4 plots the reliable and secure transmission probability versus τ_d for *Scenario 1* with different values of R_s. The correlation coefficients are generated by Clark's fading model with $v_b = v_e = 30$ km/h and $f_c = 900$ MHz. We first observe that $p_{\mathrm{rst}_1}(R_s)$ is not a monotonically decreasing function of τ_d. In particular, we find that $p_{\mathrm{rst}_1}(R_s)$ rapidly decreases before τ_d increases to 10 ms. However, when τ_d is sufficiently large, i.e., $\tau_d > 10$ ms, $p_{\mathrm{rst}_1}(R_s)$ starts to fluctuate around a certain value and does not decrease further. This observation is not surprising since the absolute values of ρ_b and ρ_e, which are generated by Clark's fading model, fluctuate in the large-delay regime. Moreover, we observe that for a fixed τ_d, $p_{\mathrm{rst}_1}(R_s)$ decreases as R_s increases, which has been explained in the descriptions of Fig. 3. Similarly, we conclude that $p_{\mathrm{rst}_2}(R_s)$ versus τ_d for *Scenario 2* has a similar conclusion. The detailed illustrations for *Scenario 2* are omitted in this section to avoid redundancy.

Fig. 5 plots the feasible security constraint versus the feasible reliability constraint for both scenarios. In this figure, $p_{co_1,LB}$, $p_{so_1,LB}$, $p_{co_2,LB}$, and $p_{so_2,LB}$ are generated from (23), (25), (36), and (38), respectively. For each scenario with specific ρ_b and ρ_e (only ρ_e in *Scenario 2*), the feasible region of ϵ and δ lies in the region above the corresponding curve. First, we observe that in both *Scenario 1* and *Scenario 2*, increasing ρ_b leads to the extension of the feasible region. Second, we observe that the feasible region in *Scenario 2* is not influenced by ρ_e, whereas in *Scenario 1*, we observe the extension in the feasible region when ρ_e increases. Third, we observe that for the same ρ_b, *Scenario 1* enables a higher reliability level than *Scenario 2*.

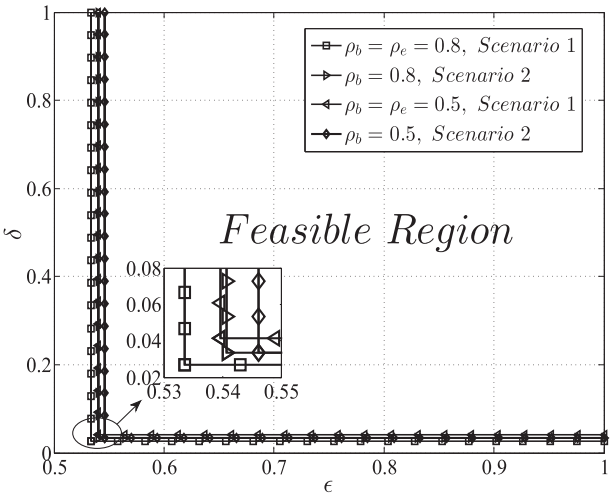

Fig. 5. Feasible security constraint versus feasible reliability constraint with outdated CSI for $\overline{\gamma}_b = 10$ dB and $\overline{\gamma}_e = 0$ dB.

However, in terms of the security level, whether *Scenario 1* performs better or not depends on the value of ρ_e. In particular, *Scenario 1* enables a higher security level when ρ_e is high (e.g., $\rho_e = 0.8$), whereas *Scenario 2* enables a higher security level when ρ_e is low (e.g., $\rho_e = 0.5$). Fourth, we observe that the feasible regions are strictly restricted at the right side of $\epsilon = 0.5$, which implies that this transmission design ignores the system reliability and can be only applied for the systems where reliability is not seen as important.

IV. Secure Transmission Design

Here, we first investigate the optimal solutions for R_s meeting (9) for each scenario; based on this, we then present numerical results to investigate the impact of the dual outage constraints on the secrecy throughput in both scenarios.

A. Optimized R_s for Scenario 1

In *Scenario 1*, the secrecy throughput is given by

$$\eta_1(R_s) = p_{tx_1}(R_s) p_{\mathrm{rst}_1}(R_s) R_s. \tag{40}$$

Mathematically, we express S_1 as

$$S_1 = \arg\max_{R_s} \quad \eta_1(R_s). \tag{41}$$

Using the mathematical software package to take the first-order derivative of $\eta_1(R_s)$ with respect to R_s, we find that $\partial\eta_1(R_s)/\partial R_s$ is first positive and then negative, which confirms that without dual outage constraints, there is a unique solution to S_1, which achieves the maximum $\eta_1(R_s)$.

Based on the feasibility for the dual outage constraints presented in (24) and (26), we express S_2 and S_3 as

$$S_2 = \{R_s | p_{co_1}(R_s) = \epsilon\} \tag{42}$$

$$S_3 = \{R_s | p_{so_1}(R_s) = \delta\} \tag{43}$$

respectively. As mentioned in Section III-A, both $p_{co_1}(R_s)$ and $p_{so_1}(R_s)$ are monotonically increasing functions of R_s, which guarantees that both (42) and (43) each have a unique solution.

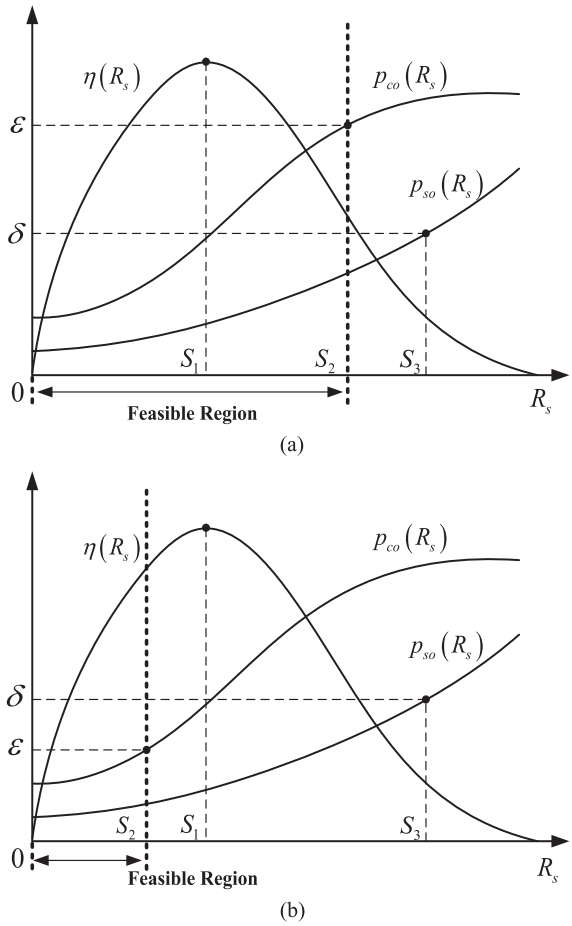

Fig. 6. Optimal R_s maximizing the secrecy throughput with dual outage constraints. (a) Case 1. (b) Case 2.

Although the closed-form solutions for S_1, S_2, and S_3 are mathematically intractable, we are able to obtain them using a numerical method, e.g., bisection method. Based on the given results, we present the optimal R_s that meets (9) in *Scenario 1* in the following proposition.

Proposition 1: The optimal R_s that maximizes the secrecy throughput *in Scenario 1*, subject to the connection and secrecy constraints, is given by

$$R_{s_1}^* = \min\{S_1, S_2, S_3\} \tag{44}$$

where S_1, S_2, and S_3 are given by (41)–(43), respectively.

Proof: By solving (41)–(43), the values of S_1, S_2, and S_3 can be obtained, as shown in Fig. 6. For a given ϵ and δ, the optimized R_s must lie within not only the feasible region determined by S_2 but the feasible region determined by S_3 as well. As such, the feasible region of R_s is $\mathbb{S} = [0, \min\{S_2, S_3\}]$. Based on $\mathbb{S}$, we obtain the optimal R_s maximizing the secrecy throughput with dual outage constraints in the following two cases.

- If $S_1 < \min\{S_2, S_3\}$, as shown in Fig. 6(a), S_1 lies within the feasible region $\mathbb{S}$. That is, the maximum $\eta_1(R_s)$ is still available in the feasible region $\mathbb{S}$, and S_1 is the unique solution. Hence, we have $R_{s_1}^* = S_1$. We highlight that in this case, the outage constraints impose no effects on the optimal solution.

- If $S_1 \geq \min\{S_2, S_3\}$, as shown in Fig. 6(b), S_1 lies beyond the feasible region $\mathbb{S}$ and cannot be treated as the solution. Moreover, we find that $\eta_1(R_s)$ is a monotonically increasing function of R_s in the feasible region $\mathbb{S}$. As such, we take $R_{s_1}^* = \min\{S_2, S_3\}$ to guarantee that the highest secrecy throughput can be obtained.

To sum up the conclusions in the aforementioned two cases, the optimal R_s maximizing the secrecy throughput with dual outage constraints in (44) can be obtained. ■

B. Optimized R_s for Scenario 2

In *Scenario 2*, the secrecy throughput is given by

$$\eta_2(R_s) = p_{tx_2}(R_s) p_{\mathrm{rst}_2}(R_s) R_s. \tag{45}$$

Mathematically, we express T_1 as

$$T_1 = \arg\max_{R_s} \quad \eta_2(R_s). \tag{46}$$

We first use the mathematical software package to take the first-order derivative of $\eta_2(R_s)$ with respect to R_s and find that $\partial\eta_2(R_s)/\partial R_s$ is first positive and then negative. This indicates that there is a unique value of R_s maximizing $\eta_2(R_s)$ subject to no outage constraints. Hence, we conclude that (46) has a unique solution.

Based on the feasibility for the dual outage constraints presented in (37) and (39), we express T_2 and T_3 as

$$T_2 = \{R_s | p_{co_2}(R_s) = \epsilon\} \tag{47}$$

$$T_3 = \{R_s | p_{so_2}(R_s) = \delta\} = \begin{cases} \log_2\left(\frac{\delta\bar{\gamma}_b}{[\exp(-1)-\delta]\bar{\gamma}_e}\right), & \delta < \exp(-1) \\ \infty, & \delta \geq \exp(-1) \end{cases} \tag{48}$$

respectively. As mentioned in Section III-B, $p_{co_2}(R_s)$ is a monotonically increasing function of R_s, which implies that (47) has a unique solution.

Despite the fact that the closed-form solutions for T_1 and T_2 are mathematically intractable, we are still able to obtain them using a numerical method, e.g., bisection method. Based on the given results, we present the optimal R_s that meets (9) in *Scenario 2* in the following proposition.

Proposition 2: The optimal R_s that maximizes the secrecy throughput in *Scenario 2*, subject to two constraints, is given by

$$R_{s_2}^* = \min\{T_1, T_2, T_3\} \tag{49}$$

where T_1, T_2, and T_3 are given by (46) and (47), respectively.

Proof: The proof is similar with the proof for ***Proposition 1***. Here, we omit the detailed proving process for brevity. ■

C. Numerical Results

Here, we present numerical results to investigate the impact of the dual outage constraints on the secrecy throughput in each scenario. Since our analytical results have been verified using Monte Carlo simulations in Section III-C, the Monte Carlo simulation points are omitted in this section to avoid unnecessary clutter.

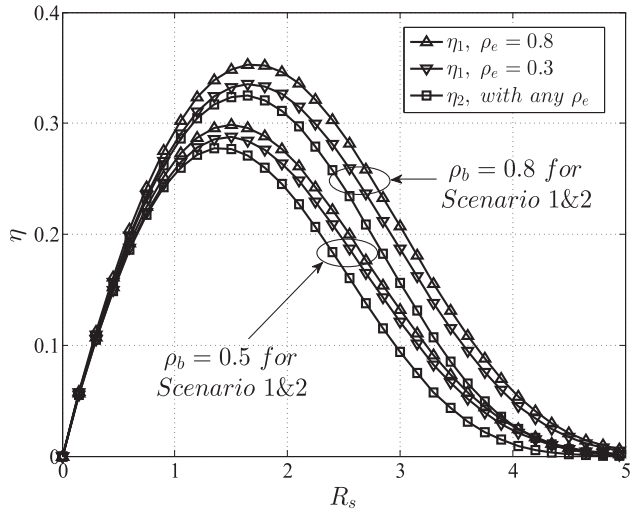

Fig. 7. Secrecy throughput subject to no outage constraints with outdated CSI for $\overline{\gamma}_b = 10$ dB and $\overline{\gamma}_e = 0$ dB.

Fig. 7 plots the secrecy throughput versus R_s for the two scenarios with different values of ρ_b and ρ_e. In this figure, we generate $\eta_1(R_s)$ and $\eta_2(R_s)$ from (40) and (45), respectively. Moreover, we do not consider the reliability and security constraints such that $\epsilon = \delta = 1$. Moreover, we do not consider the reliability and security constraints such that $\epsilon = \delta = 1$. We first observe that the secrecy throughput first increases and then decreases as R_s increases, indicating that an optimal R_s indeed exists such that the secrecy throughput is maximized. Thus, we clarify that (41) and (46) each have a unique solution. We also observe that the secrecy throughput decreases when ρ_b or ρ_e decreases. Furthermore, we observe that for the same ρ_b, the secrecy throughput in *Scenario 1* is higher than that in *Scenario 2*, even if ρ_e is fairly low (e.g., $\rho_e = 0.3$). This is due to the fact that there is a higher probability to perform transmission in *Scenario 1* than that in *Scenario 2*. Thus, *Scenario 1* offers a better secrecy throughput than *Scenario 2* without the outage constraints.

Figs. 8 and 9 plot the secrecy throughput for two scenarios versus the reliability constraint and the security constraint, respectively. We first observe that the secrecy throughput is a monotonically nondecreasing function of either constraint. We then see that a positive secrecy throughput is achieved only when the two constraints are within the feasible ranges. For example, in Fig. 8, a positive secrecy throughput is achieved when $0.534 < \epsilon \leq 1$ in *Scenario 1* and when $0.541 < \epsilon \leq 1$ in *Scenario 2*. Moreover, in Fig. 9, a positive secrecy throughput is achieved when $0.027 < \delta \leq 1$ in *Scenario 1* and when $0.034 < \delta \leq 1$ in *Scenario 2*. Notably, we find that in the specific case with $\rho_b = \rho_e = 0.8$, *Scenario 1* has a stricter security constraint and a stricter reliability constraint than *Scenario 2*. Furthermore, we observe that a constraint threshold exists such that the secrecy throughput keeps constant after the constraint exceeds the threshold. For example, it is shown in Figs. 8 and 9 that the maximum secrecy throughput in *Scenario 1* is achieved when $\epsilon \geq 0.614$ and $\delta \geq 0.081$ and the maximum secrecy throughput

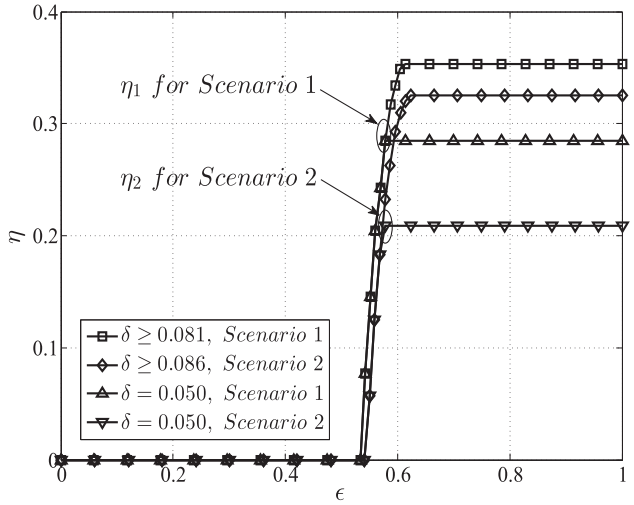

Fig. 8. Secrecy throughput versus reliability constraint with outdated CSI for $\rho_b = \rho_e = 0.8$, $\overline{\gamma}_b = 10$ dB, and $\overline{\gamma}_e = 0$ dB.

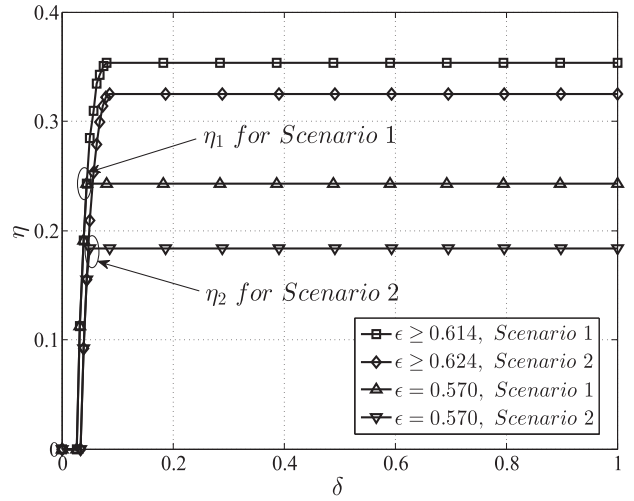

Fig. 9. Secrecy throughput versus security constraint with outdated CSI for $\rho_b = \rho_e = 0.8$, $\overline{\gamma}_b = 10$ dB, and $\overline{\gamma}_e = 0$ dB.

in *Scenario 2* is achieved when $\epsilon \geq 0.624$ and $\delta \geq 0.086$. This is due to the fact that the optimal R_s can always be used to perform data transmission with the same secrecy throughput when the constraints are higher than the thresholds.

V. Discussions

As seen in Section IV, R_s is the only controllable parameter for transmission design. Our solutions of the optimal R_s allow us to maximize the secrecy throughput subject to two constraints. We also note that the designed transmission schemes forego the reliability level, as shown in Fig. 5. This is due to the fact that in the presence of the outdated CSI, the main channel quality known at Alice tends to be higher than the instantaneous channel capacity for secure transmission. As such, this transmission design may not be suitable for the systems where the reliability is in high demand. Motivated by this, in this section, we present some discussions about the possible transmission design to improve the reliability level.

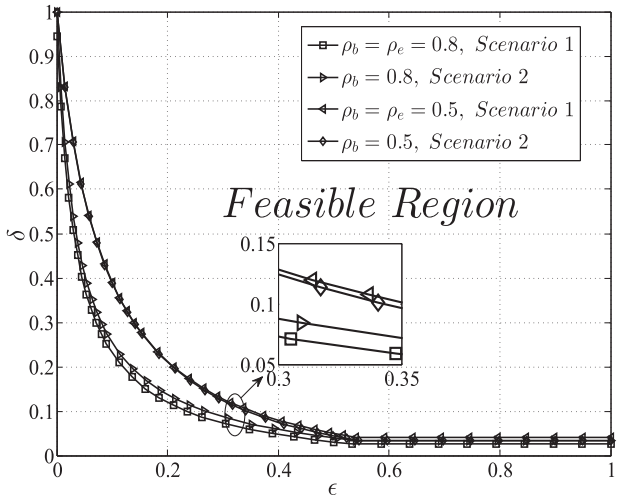

Fig. 10. Feasible security constraint versus feasible reliability constraint with outdated CSI for $\overline{\gamma}_b = 10$ dB and $\overline{\gamma}_e = 0$ dB.

Based on the aforementioned reasons, we believe that the use of $R_b = C_b$ makes the quality of the main channel overestimated. Thus, it is wise for Alice to set R_b as

$$R_b = \log_2\left(2^{R_s} + u(2^{C_b} - 2^{R_s})\right) \tag{50}$$

where $u \in [0, 1]$. Note that when $u = 1$, we have $R_b = C_b$, and when $u = 0$, we have $R_b = R_s$. It is evident from (50) that the value of R_b is within the feasible range of $[R_s, C_b]$.

By applying (50) into the system model in Section II-B and using the similar approaches in Section III, we can derive the closed-form expressions of $p_{co_1}(u, R_s)$, $p_{so_1}(u, R_s)$, $p_{co_2}(u, R_s)$, and $p_{so_2}(u, R_s)$. Thus, the lower bounds on these outage probabilities for a given u, such as $p_{co_1,LB}(u)$, $p_{so_1,LB}(u)$, $p_{co_2,LB}(u)$, and $p_{so_2,LB}(u)$, can be obtained by setting $R_s = 0$. Here, the detailed derivations are omitted for brevity. We then find that the choice of R_b, which is indicated by (50), enables a tradeoff between the feasible reliability constraint and the feasible security constraint. For example, a lower R_b leads to a lower connection outage probability but a higher secrecy outage probability. This implies that if we set a more loose reliability constraint, the security constraint becomes stricter.

To illustrate this tradeoff between the feasible reliability constraint and the feasible security constraint, Fig. 10 plots the new feasible region of the dual outage constraints for both scenarios. In this figure, the curves are generated by using the values of $p_{co_1,LB}(u)$, $p_{so_1,LB}(u)$, $p_{co_2,LB}(u)$, and $p_{so_2,LB}(u)$ at all values of u. For each scenario with fixed ρ_b and ρ_e, the feasible region of ϵ and δ lies in the region above the corresponding curve. We first observe that when u increases, the lower bound on the connection outage probability increases, but the lower bound on the secrecy outage probability decreases. For example, in *Scenario 2*, when u increases from 0 to 1, the lower bound on the connection outage probability increases from 0 to $p_{co_2,LB}$, as indicated by (36), whereas the lower bound on the secrecy outage probability decreases from 1 to $p_{so_2,LB}$, as indicated by (38). This observation is not surprising since allowing more freedom on R_b enables a

tradeoff between reliability and security. Notably, this tradeoff leads to a profound extension in the feasible region, compared with Fig. 5. We also observe the extension of the feasible region when ρ_b or ρ_e increases, which is due to the fact that the uncertainty in the main channel and the eavesdropper's channel decreases when ρ_b and ρ_e increase, respectively. This indicates that the more knowledge about the channel quality is known at Alice, the better reliability and security levels that can be achieved.

VI. Conclusion

In the presence of outdated CSI, we have adopted the on–off scheme to help perform secure transmission, under which we conducted the secrecy performance in a wiretap channel and then presented the design of wiretap coding parameters. In particular, we considered two scenarios with different assumptions on the CSI from the eavesdropper. For each scenario, we derived the transmission probability, the connection outage probability, the secrecy outage probability, and the reliable and secure transmission probability. Based on these results, we determined the optimal secrecy rates that maximize the secrecy throughput under dual connection and secrecy outage constraints. Moreover, we found that a larger feasible region of the dual outage constraints can be obtained by optimizing the codeword transmission rate.

Appendix A
Derivation of $p_{co_1}(R_s)$ in (12)

Based on (11), we formulate $p_{co_1}(R_s)$ as

$$\begin{aligned} p_{co_1}(R_s) &= \Pr\{\tilde{C}_b < C_b | C_b - C_e \geq R_s\} \\ &= \Pr\left\{\tilde{\gamma}_b < \gamma_b | \gamma_b \geq 2^{R_s}(1+\gamma_e) - 1\right\} \\ &= \frac{\Pr\left\{\bar{\gamma}_b < \gamma_b, \gamma_b \leq 2^{R_s}(1+\gamma_e) - 1\right\}}{\Pr\left\{\gamma_b \geq 2^{R_s}(1+\gamma_e) - 1\right\}}. \end{aligned} \tag{51}$$

We first re-express the numerator of $p_{co_1}(R_s)$ as

$$\begin{aligned} &\Pr\left\{\tilde{\gamma}_b < \gamma_b, \gamma_b \geq 2^{R_s}(1+\gamma_e) - 1\right\} \\ &= \underbrace{\int_0^{\infty} \underbrace{\int_{2^{R_s}(1+x)-1}^{\infty} \underbrace{\int_0^{y} f_{\tilde{\gamma}_b|\gamma_b}(z|y)dz}_{\Xi_1} f_{\gamma_b}(y)dy}_{\Xi_2} f_{\gamma_e}(x)dx}. \end{aligned} \tag{52}$$

Recall that $\tilde{\gamma}_b$ and γ_b are two correlated exponential random variables (RVs). The conditional pdf of $\tilde{\gamma}_b$ conditioned on a given γ_b is given by

$$f_{\tilde{\gamma}_b|\gamma_b}(z|y) = \frac{1}{(1-\rho_b^2)\,\bar{\gamma}_b} \exp\left(-\frac{z+\rho_b^2 y}{(1-\rho_b^2)\,\bar{\gamma}_b}\right) I_0\left(\frac{2\rho_b\sqrt{zy}}{(1-\rho_b^2)\,\bar{\gamma}_b}\right). \tag{53}$$

Substituting (53) into Ξ_1, we derive Ξ_1 as

$$\Xi_1 = 1 - Q_1\left(\sqrt{\frac{2\rho_b^2 y}{(1-\rho_b^2)\,\bar{\gamma}_b}}, \sqrt{\frac{2y}{(1-\rho_b^2)\,\bar{\gamma}_b}}\right) \tag{54}$$

where $Q_1(a,b)$ represents Marcum's Q-function [34]. We then use the series representation of Marcum's Q-function in terms of Bessel functions, which is given by

$$Q_1(a,b) = \exp\left(-\frac{a^2+b^2}{2}\right) \sum_{n=0}^{\infty} \left(\frac{a}{b}\right)^n I_n(ab) \tag{55}$$

and the expansion of Bessel function [33, eq. (8.445)], which is given by

$$I_v(z) = \sum_{k=0}^{\infty} \frac{1}{k!\Gamma(v+k+1)} \left(\frac{z}{2}\right)^{v+2k} \tag{56}$$

to obtain the series representation of Ξ_1, which yields

$$\begin{aligned} \Xi_1 = 1 - \exp\left(-\frac{(1+\rho_b^2)\,y}{(1-\rho_b^2)\,\bar{\gamma}_b}\right) &\sum_{n=0}^{\infty}\sum_{k=0}^{\infty} \frac{\rho_b^{2(n+k)}}{k!} \\ &\times \frac{1}{\Gamma(n+k+1)} \left(\frac{y}{(1-\rho_b^2)\,\bar{\gamma}_b}\right)^{n+2k}. \end{aligned} \tag{57}$$

Substituting (57) into Ξ_2, we derive Ξ_2 as

$$\begin{aligned} \Xi_2 = \exp\left(-\frac{2^{R_s}x + 2^{R_s} - 1}{\bar{\gamma}_b}\right) &- \exp\left(-\frac{2(2^{R_s}-1)}{(1-\rho_b^2)\,\bar{\gamma}_b}\right) \\ &\times \exp\left(-\frac{2^{1+R_s}x}{(1-\rho_b^2)\,\bar{\gamma}_b}\right) \sum_{n=0}^{\infty}\sum_{k=0}^{\infty} \frac{\rho_b^{2(n+k)}\left(1-\rho_b^2\right)}{k!2^{n+2k+1}} \\ &\times \frac{(n+2k)!}{(n+k)!} \sum_{m=0}^{n+2k}\sum_{q=0}^{m} \frac{(2^{R_s}-1)^{m-q} 2^{m+qR_s} x^q}{q!(m-q)!\left((1-\rho_b^2)\,\bar{\gamma}_b\right)^m}. \end{aligned} \tag{58}$$

Substituting (58) into (52) and solving the resultant integrals, the numerator of $p_{co_1}(R_s)$ is obtained. We also note that the denominator of $p_{co_1}(R_s)$ is given by (10). Therefore, we obtain $p_{co_1}(R_s)$ in (12).

Appendix B
Derivation of $p_{so_1}(R_s)$ in (14)

Based on (13), we formulate $p_{so_1}(R_s)$ as

$$\begin{aligned} p_{so_1}(R_s) &= \Pr\{C_b - R_s < \tilde{C}_e | C_b - C_e \geq R_s\} \\ &= \Pr\left\{\gamma_b < 2^{R_s}(1+\tilde{\gamma}_e) - 1 \,\middle|\, \gamma_b \geq 2^{R_s}(1+\gamma_e) - 1\right\} \\ &= \frac{\Pr\left\{\gamma_b < 2^{R_s}(1+\tilde{\gamma}_e) - 1, \gamma_b \geq 2^{R_s}(1+\gamma_e) - 1\right\}}{\Pr\left\{\gamma_b \geq 2^{R_s}(1+\gamma_e) - 1\right\}}. \end{aligned} \tag{59}$$

We re-express the numerator of $p_{so_1}(R_s)$ as

$$\begin{aligned} &\Pr\left\{\gamma_b < 2^{R_s}(1+\tilde{\gamma}_e) - 1, \gamma_b \geq 2^{R_s}(1+\gamma_e) - 1\right\} \\ &= \Pr\left\{\tilde{\gamma}_e > 2^{-R_s}(1+\gamma_b) - 1, \gamma_e \leq 2^{-R_s}(1+\gamma_b) - 1\right\} \\ &= \int_{2^{R_s}-1}^{\infty} \underbrace{\int_0^{2^{-R_s}(1+x)-1} \Phi_1 f_{\gamma_e}(y)dy}_{\Phi_2} f_{\gamma_b}(x)dx \end{aligned} \tag{60}$$

where Φ_1 is

$$\Phi_1 = \int_{2^{-R_s}(1+x)-1}^{\infty} f_{\tilde{\gamma}_e|\gamma_e}(z|y)dz. \tag{61}$$

Recall that $\tilde{\gamma}_e$ and γ_e are two correlated exponential RVs. The conditional pdf of $\tilde{\gamma}_e$ conditioned on a given γ_e is given by

$$f_{\tilde{\gamma}_e|\gamma_e}(z|y) = \frac{1}{(1-\rho_e^2)\,\bar{\gamma}_e} \exp\left(-\frac{z+\rho_e^2 y}{(1-\rho_e^2)\,\bar{\gamma}_e}\right) \times I_0\left(\frac{2\rho_e\sqrt{zy}}{(1-\rho_e^2)\,\bar{\gamma}_e}\right). \quad (62)$$

We then substitute (62) into (61) to derive Φ_1 as

$$\Phi_1 = Q_1\left(\sqrt{\frac{2\rho_e^2 y}{(1-\rho_e^2)\,\bar{\gamma}_e}}, \sqrt{\frac{2^{1-R_s}(x+1)-2}{(1-\rho_e^2)\,\bar{\gamma}_e}}\right). \quad (63)$$

With the help of (55) and (56), the series representation of Φ_1 is obtained as

$$\Phi_1 = \exp\left(-\frac{\rho_e^2 y + 2^{-R_s}x + 2^{-R_s}-1}{(1-\rho_e^2)\,\bar{\gamma}_e}\right) \sum_{n=0}^{\infty}\sum_{k=0}^{\infty} \frac{1}{k!} \times \frac{\rho_e^{2(n+k)} y^{n+k}(2^{-R_s}x + 2^{-R_s}-1)^k}{\Gamma(n+k+1)((1-\rho_e^2)\,\bar{\gamma}_e)^{n+2k}}. \quad (64)$$

Substituting (64) into Φ_2, we obtain the series representation of Φ_2 as

$$\Phi_2 = \exp\left(-\frac{x+1-2^{R_s}}{(1-\rho_e^2)\,2^{R_s}\bar{\gamma}_e}\right) \sum_{n=0}^{\infty}\sum_{k=0}^{\infty} \frac{\rho_e^{2(n+k)}\left(1-\rho_e^2\right)}{k!((1-\rho_e^2)\,\bar{\gamma}_e)^k} \times \left(\frac{x+1-2^{R_s}}{2^{R_s}}\right)^k \left[1-\exp\left(-\frac{x+1-2^{R_s}}{(1-\rho_e^2)\,2^{R_s}\bar{\gamma}_e}\right) \times \sum_{m=0}^{n+k}\frac{1}{m!}\left(\frac{x+1-2^{R_s}}{(1-\rho_e^2)\,2^{R_s}\bar{\gamma}_e}\right)^m\right]. \quad (65)$$

Finally, we substitute (65) into (60) and solve the resultant integrals to obtain the numerator of $p_{so_1}(R_s)$. Hence, $p_{so_1}(R_s)$ in (14) can be obtained.

APPENDIX C
DERIVATION OF $p_{\mathrm{rst}_1}(R_s)$ IN (18)

Based on (17), we formulate $p_{\mathrm{rst}_1}(R_s)$ as

$$\begin{aligned} &p_{\mathrm{rst}_1}(R_s) \\ &= \Pr\{\tilde{C}_b \geq C_b, C_b - R_s \geq \tilde{C}_e | C_b - C_e \geq R_s\} \\ &= \Pr\left\{\tilde{\gamma}_b \geq \gamma_b, \gamma_b \geq 2^{R_s}(1+\tilde{\gamma}_e)-1 | \gamma_b \geq 2^{R_s}(1+\gamma_e)-1\right\} \\ &= \frac{\Pr\left\{\tilde{\gamma}_b \geq \gamma_b, \gamma_b \geq 2^{R_s}(1+\tilde{\gamma}_e)-1, \gamma_b \geq 2^{R_s}(1+\gamma_e)-1\right\}}{\Pr\left\{\gamma_b \geq 2^{R_s}(1+\gamma_e)-1\right\}}. \end{aligned} \quad (66)$$

By re-expressing the numerator of $p_{\mathrm{rst}_1}(R_s)$, we obtain

$$\Pr\left\{\tilde{\gamma}_b \geq \gamma_b, \tilde{\gamma}_e \leq \frac{1+\gamma_b}{2^{R_s}} - 1, \gamma_e \leq \frac{1+\gamma_b}{2^{R_s}} - 1\right\} = \int_{2^{R_s}-1}^{\infty} \Delta_1 \Delta_2 f_{\gamma_b}(x)dx \quad (67)$$

where Δ_1 is

$$\Delta_1 = \Pr\{\tilde{\gamma}_b \geq x\} = \int_x^{\infty} f_{\tilde{\gamma}_b|\gamma_b}(w|x)dw \quad (68)$$

and Δ_2 is

$$\Delta_2 = \Pr\left\{\tilde{\gamma}_e \leq 2^{-R_s}(1+x)-1, \gamma_e \leq 2^{-R_s}(1+x)-1\right\} = \int_0^{2^{-R_s}(1+x)-1}\int_0^{2^{-R_s}(1+x)-1} f_{\tilde{\gamma}_e|\gamma_e}(z|y)dz f_{\gamma_e}(y)dy. \quad (69)$$

With the help of Ξ_1 in Appendix A and Φ_2 in Appendix B, we obtain the series representations of Δ_1 and Δ_2 as

$$\Delta_1 = 1 - \Xi_1 \quad (70)$$

$$\Delta_2 = 1 - \exp\left(-\frac{2^{-R_s}x + 2^{-R_s}-1}{\bar{\gamma}_e}\right) - \Phi_2 \quad (71)$$

where Ξ_1 is given by (57), and Φ_2 is given by (65).

Finally, substituting (70) and (71) into (67) and solving for the resultant integrals, the numerator of $p_{\mathrm{rst}_1}(R_s)$ is obtained. Using (10), $p_{\mathrm{rst}_1}(R_s)$ in (18) can be obtained.

REFERENCES

[1] H. V. Poor, "Information and inference in the wireless physical layer," *IEEE Wireless Commun.*, vol. 19, no. 1, pp. 40–47, Feb. 2012.

[2] B. Schneier, "Cryptographic design vulnerabilities," *Computer*, vol. 31, no. 9, pp. 29–33, Sep. 1998.

[3] X. Zhou, L. Song, and Y. Zhang, *Physical Layer Security in Wireless Communications*. Boca Raton, FL, USA: CR, 2013.

[4] N. Yang *et al.*, "Safeguarding 5G wireless communication networks using physical layer security," *IEEE Commun. Mag.*, vol. 53, no. 4, pp. 20–27, Apr. 2015.

[5] C. E. Shannon, "Communication theory of secrecy systems," *Bell Syst. Tech. J.*, vol. 28, no. 4, pp. 656–715, Oct. 1949.

[6] A. D. Wyner, "The wire-tap channel," *Bell Syst. Tech. J.*, vol. 54, no. 8, pp. 1355–1387, Oct. 1975.

[7] I. Csiszàr and J. Körner, "Broadcast channels with confidential messages," *IEEE Trans. Inf. Theory*, vol. IT-24, no. 3, pp. 339–348, May 1978.

[8] S. K. Leung-Yan-Cheong and M. E. Hellman, "The Gaussian wire-tap channel," *IEEE Trans. Inf. Theory*, vol. IT-24, no. 4, pp. 451–456, Jul. 1978.

[9] H. Alves, R. D. Souza, M. Debbah, and M. Bennis, "Performance of transmit antenna selection physical layer security schemes," *IEEE Signal Process. Lett.*, vol. 19, no. 6, pp. 372–375, Jun. 2012.

[10] N. Yang, P. L. Yeoh, M. Elkashlan, R. Schober, and I. B. Collings, "Transmit antenna selection for security enhancement in MIMO wiretap channels," *IEEE Trans. Commun.*, vol. 61, no. 1, pp. 144–154, Jan. 2013.

[11] N. Yang, P. L. Yeoh, M. Elkashlan, R. Schober, and J. Yuan, "MIMO wiretap channels: Secure transmission using transmit antenna selection and receive generalized selection combining," *IEEE Commun. Lett.*, vol. 17, no. 9, pp. 1754–1757, Sep. 2013.

[12] N. Yang, H. A. Suraweera, I. B. Collings, and C. Yuen, "Physical layer security of TAS/MRC with antenna correlation," *IEEE Trans. Inf. Forensics Security*, vol. 8, no. 1, pp. 254–259, Jan. 2013.

[13] J. Hu, Y. Cai, N. Yang, and W. Yang, "A new secure transmission scheme with outdated antenna selection," *IEEE Trans. Inf. Forensics Security*, vol. 10, no. 11, pp. 2435–2446, Nov. 2015.

[14] X. Zhou and M. R. McKay, "Secure transmission with artificial noise over fading channels: Achievable rate and optimal power allocation," *IEEE Trans. Veh. Technol.*, vol. 59, no. 8, pp. 3831–3842, Oct. 2010.

[15] A. Mukherjee and A. L. Swindlehurst, "Robust beamforming for security in MIMO wiretap channels with imperfect CSI," *IEEE Trans. Signal Process.*, vol. 59, no. 1, pp. 351–361, Jan. 2011.

[16] J. M. Taylor, M. Hempel, H. Sharif, S. Ma, and Y. Yang, "Impact of channel estimation errors on effectiveness of eigenvector-based jamming for physical layer security in wireless networks," in *Proc. IEEE CAMAD Workshop*, Kyoto, Japan, Jun. 2011, pp. 122–126.

[17] T. Y. Liu, S. C. Lin, T. H. Chang, and Y. W. P. Hong, "How much training is enough for secrecy beamforming with artificial noise," in *Proc. IEEE Int. Conf. Commun.*, Ottawa, ON, Canada, Jun. 2012, pp. 4782–4787.

[18] M. Pei, J. Wei, K. K. Wong, and X. Wang, "Masked beamforming for multiuser MIMO wiretap channels with imperfect CSI," *IEEE Trans. Wireless Commun.*, vol. 11, no. 2, pp. 544–549, Feb. 2012.

[19] B. He and X. Zhou, "Secrecy on–off transmission design with channel estimation errors," *IEEE Trans. Inf. Forensics Security*, vol. 8, no. 12, pp. 1923–1936, Dec. 2013.
[20] S. Bashar, Z. Ding, and Y. Li, "On secrecy of codebook-based transmission beamforming under receiver limited feedback," *IEEE Trans. Wireless Commun.*, vol. 10, no. 4, pp. 1212–1223, Apr. 2011.
[21] S. C. Lin, T. H. Chang, Y. L. Liang, Y. W. P. Hong, and C. Y. Chi, "On the impact of quantized channel feedback in guaranteeing secrecy with artificial noise: The noise leakage problem," *IEEE Trans. Wireless Commun.*, vol. 10, no.3, pp. 901–915, Mar. 2011.
[22] L. Sun and S. Jin, "On the ergodic secrecy rate of multiple-antenna wiretap channels using artificial noise and finite-rate feedback," in *Proc. IEEE Int. Symp. Pers., Indoor, Mobile Radio Commun.*, Toronto, ON, Canada, Sep. 2011, pp. 1–5.
[23] Z. Rezki, A. Khisti, and M. S. Alouini, "On the ergodic secret message capacity of the wiretap channel with finite-rate feedback," in *Proc. IEEE Int. Symp. Inf. Theory*, Cambridge, MA, USA, Jul. 2012, pp. 239–243.
[24] X. Zhang, M. R. McKay, X. Zhou, and R. W. Heath, Jr., "Artificial-noise-aided secure multi-antenna transmission with limited feedback," *IEEE Trans. Wireless Commun.*, vol. 14, no. 5, pp. 2742–2754, May 2015.
[25] Y. Yang, W. Wang, H. Zhao, and L. Zhao, "Transmitter beamforming and artificial noise with delayed feedback: Secrecy rate and power allocation," *J. Commun. Netw.*, vol. 14, no. 4, pp. 374–384, Aug. 2012.
[26] N. S. Ferdinand, D. B. Costa, and M. Latva-aho, "Effects of outdated CSI on the secrecy performance of MISO wiretap channels with transmit antenna selection," *IEEE Commun. Lett.*, vol. 17, no. 5, pp. 864–867, May 2013.
[27] P. K. Gopala, L. Lai, and H. E. Gamal, "On the secrecy capacity of fading channels," *IEEE Trans. Inf. Theory*, vol. 54, no. 10, pp. 4687–4698, Oct. 2008.
[28] X. Zhou, M. R. McKay, B. Maham, and A. Hjørungnes, "Rethinking the secrecy outage formulation: A secure transmission design perspective," *IEEE Commun. Lett.*, vol. 15, no. 3, pp. 302–304, Mar. 2011.
[29] Y. Liang, H. V. Poor, and S. Shamai, "Secure communication over fading channels," *IEEE Trans. Inf. Theory*, vol. 54, no. 6, pp. 2470–2492, Jun. 2008.
[30] A. Khisti and G. Wornell, "Secure transmission with multiple antennas—I: The MISOME wiretap channel," *IEEE Trans. Inf. Theory*, vol. 56, no.7, pp. 3088–3104, Jul. 2010.
[31] A. Khisti and G. Wornell, "Secure transmission with multiple antennas—II: The MIMOME wiretap channel," *IEEE Trans. Inf. Theory*, vol. 56, no. 11, pp. 5515–5532, Nov. 2010.
[32] D. S. Michalopoulos, H. A. Suraweera, G. K. Karagiannidis, and R. Schober, "Amplify-and-forward relay selection with outdated channel estimates," *IEEE Trans. Commun.*, vol. 60, no. 5, pp. 1278–1290, May 2012.
[33] I. S. Gradshteyn and I. M. Ryzhik, *Table of Integrals, Series and Products*, 7th ed. New York, NY, USA: Academic, 2007.
[34] J. I. Marcum, *Table of Q Functions*. Santa Monica, CA, USA: Rand, 1950.

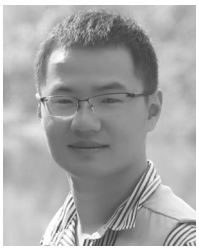

Jianwei Hu (S'14) received the B.S. degree in communication engineering from the College of Communications Engineering, PLA University of Science and Technology, Nanjing, China, in 2012, where he is currently working toward the Ph.D. degree in communications and information systems.

His research interests include multiple-input–multiple-output systems, cooperative communications, and network security.

Weiwei Yang (S'08–M'12) received the B.S., M.S., and Ph.D. degrees from the College of Communications Engineering, PLA University of Science and Technology, Nanjing, China, in 2003, 2006, and 2011, respectively.

His research interests include orthogonal frequency-domain multiplexing systems, signal processing in communications, cooperative communications, cognitive networks, and network security.

Nan Yang (S'09–M'11) received the B.S. degree in electronics from China Agricultural University, Beijing, China, in 2005 and the M.S. and Ph.D. degrees in electronic engineering from the Beijing Institute of Technology, in 2007 and 2011, respectively.

He is currently a Future Engineering Research Leadership Fellow and a Lecturer with the Research School of Engineering, Australian National University, Canberra, Australia. Prior to this, he was a Postdoctoral Research Fellow with the University of New South Wales (UNSW), Sydney, Australia, from 2012 to 2014; a Postdoctoral Research Fellow with the Commonwealth Scientific and Industrial Research Organization, Canberra, from 2010 to 2012; and a visiting Ph.D. student with the UNSW from 2008 to 2010. His general research interests include communications theory and signal processing, with specific interests in collaborative networks, network security, resource management, massive multiantenna systems, millimeter-wave communications, and molecular communications.

Dr. Yang received the IEEE Communications Society Asia-Pacific Outstanding Young Researcher Award in 2014, the Exemplary Reviewer Certificate from the IEEE WIRELESS COMMUNICATIONS LETTERS in 2014, the Exemplary Reviewer Certificate from the IEEE COMMUNICATIONS LETTERS in 2012 and 2013, and the Best Paper Award at the IEEE 77th Vehicular Technology Conference in 2013. He serves as an Editor for the TRANSACTIONS ON EMERGING TELECOMMUNICATIONS TECHNOLOGIES. He also served as a Guest Editor for the Special Issue on "Enabling Nano-Networking via Molecular Communications" of the TRANSACTIONS ON EMERGING TELECOMMUNICATIONS TECHNOLOGIES and as a Guest Editor for the Special Issue on "Physical Layer Security for Emerging Wireless Networks: From Theory to Practice" of *Physical Communication*.

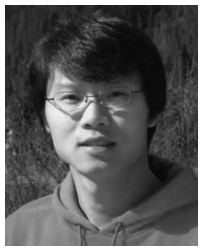

Xiangyun Zhou (S'08–M'11) received the B.E. (Hons.) degree in electronics and telecommunications engineering and the Ph.D. degree in telecommunications engineering from the Australian National University, Canberra, Australia, in 2007 and 2010, respectively.

From 2010 to 2011, he was a Postdoctoral Fellow with The University Graduate Center (UNIK), University of Oslo, Oslo, Norway. In 2011, he joined the Australian National University, where he is currently a Senior Lecturer. His research interests include communication theory and wireless networks.

Dr. Zhou currently serves on the Editorial Board of the IEEE TRANSACTIONS ON WIRELESS COMMUNICATIONS and the IEEE COMMUNICATIONS LETTERS. He also served as a Guest Editor for the IEEE COMMUNICATIONS MAGAZINE's feature topic on wireless physical-layer security in 2015. He was a Cochair of the 2014 and 2015 IEEE International Communications Conference Workshop on Wireless Physical Layer Security. From 2013 to 2014, he was the Chair of the ACT Chapter of the IEEE Communications and the Signal Processing Societies. He received the Best Paper Award at the 2011 IEEE International Communications Conference.

Yueming Cai (M'05–SM'12) received the B.S. degree in physics from Xiamen University, Xiamen, China, in 1982 and the M.S. degree in microelectronics engineering and the Ph.D. degree in communications and information systems from Southeast University, Nanjing, China, in 1988 and 1996, respectively.

His current research interests include multiple-input–multiple-output systems, orthogonal frequency-division multiplexing systems, signal processing in communications, cooperative communications, and wireless sensor networks.